JOURNAL OF CATALYSIS 109, 252–262 (1988)

UV–Visible Spectroscopic Investigations of the Modified Claus Reaction on NaX Zeolite Catalysts

HELLMUT G. KARGE, MAREK ŁANIECKI,[1] AND MARIA ZIOŁEK[1]

Fritz-Haber-Institut der Max-Planck-Gesellschaft, Faradayweg 4-6, 1000 Berlin 33 (Dahlem), Federal Republic of Germany

Received November 17, 1986; revised August 31, 1987

Interaction of SO_2 and H_2S, i.e., the Claus reaction, on faujasite-type zeolite catalysts was studied by combined UV–visible and IR spectroscopy. Reactivity of HSO_3^-, formed by chemisorption of SO_2, and HS^-, formed by dissociative adsorption of H_2S, was confirmed. An effect of thermal treatment after preadsorption of H_2S on the kinetics of interaction with subsequently admitted SO_2 was observed. $S_2O_4^{2-}$, S_2^{2-}, and c-S_8 as well as polymeric sulfur were identified as intermediates and product species. The same bands, ascribed to intermediates and products, were observed when H_2S was oxidized by oxygen instead of SO_2. © 1988 Academic Press, Inc.

1. INTRODUCTION

In the classic Claus reaction, hydrogen sulfide is oxidized by oxygen according to Eq. (1).

$$2H_2S + O_2 \rightarrow S_2 + 2H_2O \qquad (1)$$

$$(n/2)S_2 \rightarrow S_n \ (n = 3, 4, \ldots, 8)$$

The modified Claus process first converts part of the H_2S to SO_2 and then oxidizes the rest of H_2S by SO_2, according to Eq. (2).

$$2H_2S + SO_2 \rightarrow \tfrac{3}{2}S_2 + 2H_2O \qquad (2)$$

$$(n/2)S_2 \rightarrow S_n \ (n = 3, 4, \ldots, 8)$$

Both processes employ alumina or bauxite as catalysts. However, even though zeolites probably never will replace these well-established materials, they are useful model catalysts for the Claus reaction. Their crystal chemistry has been thoroughly investigated by many workers and can be modified by clear-cut procedures, e.g., via ion exchange. Some specific features of reactant adsorption were first discovered with zeolite/SO_2 or zeolite/H_2S systems.

Adsorption of SO_2 and H_2S both on alumina and zeolites has been widely studied. Mainly IR spectroscopy has been applied, starting with the pioneering work of Deo, Dalla Lana, and Habgood (*1*). Subsequently, contributions came from several groups, e.g., Slager and Amberg (*2*), Förster *et al.* (*3–5*), Karge *et al.* (*6–9*), Lavalley *et al.* (*10–15*) and Datta *et al.* (*16–18*). In particular, Förster *et al.* (*3*) and Karge *et al.* (*6–7*) provided evidence for dissociative adsorption of H_2S on zeolite NaA and faujasite-like zeolites, respectively. With respect to SO_2 adsorption, one essential result of the IR study by Chang (*19*) was the detection of a chemisorbed species characterized by a low-frequency band (LFB), viz., at about 1070 cm^{-1} in the case of alumina. The band was attributed to a sulfite-like structure. Karge *et al.* confirmed the existence of that species on alumina (*20–22*) as well as on zeolites (*23*) and showed by *in situ* experiments that these low-frequency species were the only reactive entities detectable via IR on a working Claus catalyst. Also, in a FTIR study by Datta *et al.* (*17*) this LFB structure was identified, among other adsorbate species.

However, the structure of the LFB species, derived from adsorbed SO_2, remained

---

[1] On leave from the Faculty of Chemistry, Adam Mickiewicz University, Poznań, Poland.

0021-9517/88 $3.00

a matter of debate. While Chang (*19*), Lavalley *et al.* (*11*), and Datta *et al.* (*17*) postulated a sulfite-like structure, Karge *et al.* (*9, 20*) suggested a correlation of the low-frequency bands (1070 cm^{-1} on alumina, 1240 cm^{-1} on zeolites) with the existence of SO_2^- anion radicals. These radicals have been identified by EPR in a number of investigations of SO_2 adsorption on alumina and zeolites (*20, 24–30*). However, Karge *et al.* (*22, 23, 31*) showed later by a combined IR/EPR reinvestigation that no correlation between the LFB species of adsorbed SO_2 and the SO_2^- seems to exist. Moreover, very recent UV/vis spectroscopic studies by the same group (*32*) indicated a strong probability that those low-frequency IR bands were due to the formation of HSO_3^- molecules upon adsorption of SO_2 on alumina as well as on zeolites. The particular structure of the respective adsorbate complex, however, might depend on the surroundings and be different on alumina and zeolites.

Simultaneously, the UV/vis study demonstrated the value of these techniques when applied to adsorption measurements on solid catalysts and, particularly, when combined with IR spectroscopy. H_2S adsorption onto faujasite-like zeolites was monitored by UV/vis spectroscopy and provided evidence that complete dissociation of H_2S might occur on particular sites of the catalysts, whereby nonreactive S^{2-} ions form (*33*). Therefore, application of a combination of UV/vis and IR spectroscopic techniques to the investigation of the Claus reaction seemed promising. The present paper reports results of experiments in which the interaction of SO_2 adsorbed on NaX zeolite with H_2S and vice versa was traced by UV, vis, and IR, and particular attention was paid to the occurrence and reactivity of intermediates and product species.

2. EXPERIMENTAL

NaX was provided by Union Carbide (lot no. 2565330); the unit cell composition according AAS analysis was $Na_{89}Al_{84}Si_{107}O_{384}$ after five repeated exchanges with 0.1 *M* NaCl solution. Thin self-supporting wafers (3 mg cm^{-2}) were used. H_2S (99.5 vol%), SO_2 (99.98 vol%), and O_2 (99.8 vol%) were purchased from Messer–Griesheim, Düsseldorf. UV/vis measurements were carried out at room temperature in transmission mode with a Perkin–Elmer/Hitachi spectrometer Model 556; IR spectra were obtained by a Perkin–Elmer spectrometer Model 225. The cell, which allowed measurements in the UV/vis and IR regions with one and the same sample, is described elsewhere (*33*). It could be connected to a high-vacuum and gas-dosing system. Amounts adsorbed were evaluated from the pressure change when the gases were admitted from calibrated reservoirs to the known cell volume. Adsorbate pressures were monitored by a MKS Baratron. Prior to gas admission, the sample was slowly (5 K min^{-1}) heated at 10^{-5} Pa to 625 K and maintained at this temperature for 12 h. For a more detailed description of the procedure see Ref. (*33*).

3. RESULTS AND DISCUSSION

3.1. SO_2 Preadsorption at Room Temperature Followed by H_2S Interaction at Room Temperature

When 0.73 mmol g^{-1} SO_2 was adsorbed onto an activated NaX wafer and very weakly held SO_2 was removed by subsequent short evacuation at room temperature (r.t.), spectrum 1 of Fig. 1 appeared. It exhibited the expected band at 280 nm and a shoulder around 250 nm, which were due to physically adsorbed SO_2 and $S_2O_5^{2-}$, respectively (*32*). The band of chemisorbed HSO_3^- at 215 nm is, at this high coverage, masked by the SO_2 and $S_2O_5^{2-}$ signals (*32*). Subsequent admission of H_2S at r.t. caused a band at 320 nm and a shoulder around 400 nm to appear (curves 2, 3, and 4 in Fig. 1). Remarkably, no significant decrease in absorbance around 280 nm was observed as one would expect as a result of reaction

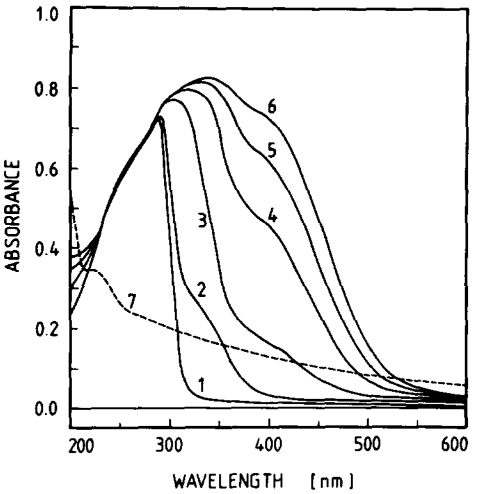

FIG. 1. UV/vis spectra after preadsorption of SO_2 and subsequent admission of H_2S, at room temperature (r.t.). (1), Preadsorption of 0.73 mmol g^{-1}, followed by short evacuation; (2) through (4), after admission of 0.08, 0.96, and 1.47 mmol g^{-1} H_2S, respectively; (5) and (6), 15 min and 1 h after last admission, respectively; (7), after desorption at 523 K.

between preadsorbed SO_2 and H_2S admitted. This seemed to indicate that reaction products form which absorb in the same UV region as preadsorbed SO_2 (see below). At r.t., formation of the products of interaction between SO_2 and H_2S slackened when higher portions of H_2S were admitted; the broad bands around 320–330 and 400 nm continued to grow even when considerable time had elapsed after the last H_2S admission (see curves 5 and 6 in Fig. 1).

Evacuation at r.t., following the SO_2/H_2S interaction, removed a significant amount of weakly held material from the zeolite wafer, and a spectrum close to that of curve 3 in Fig. 1 remained. Subsequent evacuation at 393 K did not cause a noticeable change. Thus, the 320- and 400-nm species were relatively strongly adsorbed. Desorption at 523 K was needed to remove all the bands but a small absorption was then revealed around 220 nm, indicating that some chemisorbed HSO_3^- was still left on the surface (Fig. 1, curve 7).

The product species which gave rise to the bands at 320 nm and around 400 nm could be observed more distinctly when difference spectra were derived. The set of experiments of Fig. 2 started with preadsorption of 0.24 mmol g^{-1} SO_2 at r.t. (see the inset), reproducing the features which were reported in Ref. (*32*): bands at 215 (chemisorbed HSO_3^-), 250 ($S_2O_5^{2-}$), and 280 nm (physically adsorbed SO_2). This spectrum was stored and subtracted from each of the subsequent spectra, which were obtained after H_2S admission.

These difference spectra exhibited two prominent well-resolved bands at 320 and 385 nm, respectively. The latter band appeared in Fig. 1 merely as a broad shoulder around 400 nm. Under the present conditions (r.t.), the reaction was completed already at a ratio H_2S (admitted)/SO_2 (preadsorbed) = 1. Admission of H_2S in excess of this ratio did not change the spectrum further (Fig. 2, curves 5–7). Like the results presented in Fig. 1, the difference spectra do not show a significant decrease in ab-

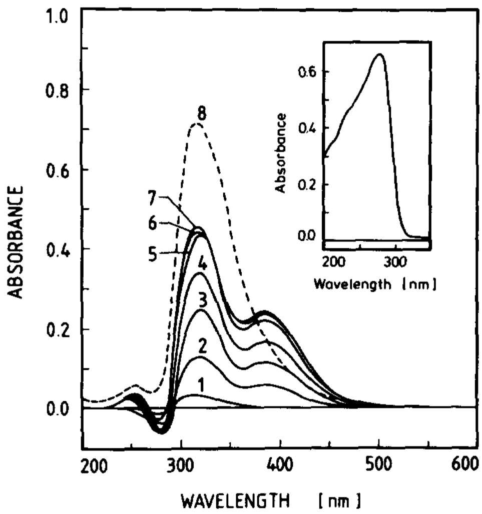

FIG. 2. UV/vis difference spectra after preadsorption of SO_2 and subsequent admission of H_2S, at r.t. Inset: spectrum after adsorption of 0.24 mmol g^{-1} SO_2 onto NaX (compare Fig. 1, line 1); subtracted after subsequent H_2S admission; (1) through (7), after admission of 0.05, 0.09, 0.14, 0.19, 0.24, 0.28, and 0.33 mmol g^{-1} H_2S, resepectively; (8) after subsequent admission of 0.24 mmol g^{-1} SO_2.

sorbance around 280 nm, which should have occurred because of the consumption of SO_2. As a result of progressive SO_2 conversion one would expect a corresponding "negative" band at about 280 nm since the original spectrum of preadsorbed SO_2 (inset) is subtracted with each scan. However, only a small negative difference band appeared. As mentioned before, the most straightforward explanation is that reaction products form which also absorb around 280 nm and thus compensate almost completely for the expected decrease of absorbance when SO_2 is converted.

The small bands around 250 nm in the spectra of Fig. 2 are most probably due to S^{2-} ions; these result from complete dissociation of H_2S at particularly strong centers (*33*). All of the reaction products formed during the experiments of Fig. 2 were relatively strongly held, since evacuation at r.t. did not cause any change of spectrum 7.

As a result of the experiments described, three bands should be assigned to products of the reaction between preadsorbed SO_2 and subsequently admitted H_2S, viz., bands at 280, 320, and 385 nm.

A band at 380 nm has been observed in the spectra of sulfur-doped sodalite and ascribed to S_2^2 ions (*34–36*). Therefore, and because it fits readily into a proposed reaction scheme (see below), the band at 385 nm in Figs. 1 and 2 is tentatively assigned to S_2^{2-} ions. The shift by 5 nm may reflect the interaction of S_2^{2-} with zeolite surface sites.

According to data reported in the literature, a band around 320 nm can be assigned to either S_4^{2-} (*37, 38*), S_4^{2-} (*39*), or c-S_8 (*40*). However, if the above assignment of the 385-nm band to S_2^{2-} is correcct, S_4^{2-} ions cannot be responsible for the 320-nm band. This conclusion is drawn from the observation that the band at 320 nm increased further when the sample, after preadsorption of SO_2 and treatment with H_2S, was again contacted with SO_2 (see spectrum 8 in Fig. 2). Simultaneously, the band at 385 nm decreased in intensity and finally disappeared from the spectrum. Obviously, the species which gave rise to the 385-nm band, i.e., S_2^{2-}, were reactive toward SO_2. But the reaction between S_2^{2-} and SO_2 cannot lead to S_4^{2-}, whereas $S_2O_4^{2-}$ indeed may be formed from these two species (see Eq. 3 of the scheme given below).

Calculations and UV measurements have shown that the thermodynamically most stable sulfur species, i.e., c-S_8, exhibits a band at 320 nm (*40–42*). Sulfur species (c-S_8) should occur as final product species of SO_2 and H_2S interaction and, therefore, might well contribute to the 320 nm band.

Similarly, sulfur species are most probably responsible for the growth of a product band around 280 nm, which compensates for the expected decrease in absorbance of the 280-nm band of SO_2 in Figs. 1 and 2 (see above). In fact, Meyer *et al.* (*41, 44*) observed bands at 260–270 nm and a shoulder at 280 nm when they investigated solutions of S_8 or polymeric sulfur in isopentane/cyclohexane via UV spectroscopy.

Finally, the existence of both chemisorbed HSO_3^- and physically adsorbed SO_2 on NaX after contact with SO_2 has been well established via UV spectroscopy (*32*). Occurrence of HS^- on faujasite-like zeolites upon H_2S adsorption has been demonstrated by IR spectroscopy (*33*). Thus, all the available spectroscopic data are in agreement with the suggestion that upon reaction of SO_2 and H_2S on NaX at r.t., $S_2O_4^{2-}$ and sulfur form according to the following reaction scheme, which also involves the intermediates S_2^{2-} and HS^-:

$$2HSO_3^- + H_2S \rightarrow S_2O_4^{2-} + S + 2H_2O \qquad (3)$$

$$2HSO_3^- + 2HS^- \rightarrow S_2O_4^{2-} + S_2^{2-} + 2H_2O \qquad (4)$$

$$S_2^{2-} + 2SO_2 \rightarrow S_2O_4^{2-} + 2S. \qquad (5)$$

3.2. SO_2 Preadsorption at 393 K Followed by H_2S Interaction at 393 K

Since the zeolite wafers reached a temperature of about 375 K when exposed to the IR beam (*48*), in subsequent experiments reactant admission was carried out at 393 K. This measure rendered the comparison of UV and IR results more reliable. After the spectrum of the activated NaX sample was scanned, a new baseline was established. The NaX wafer was then loaded at r.t. with 0.38 mmol g^{-1} SO_2 which was about half of the ultimate uptake. Subsequently, the cell was closed and the system NaX/SO_2 thermally treated at 393 K. This temperature was maintained for 1 h. Thereafter, the cell was cooled to r.t. and the SO_2 spectrum was scanned (spectrum 1 in Fig. 3). The sample was heated again to 393 K. H_2S was admitted and reacted at this temperature for 5 min. The cell was cooled, and the next spectrum was run (spectrum 2 in Fig. 3). The same procedure was applied to obtain all the other spectra of Fig. 3 and Fig. 5.

The SO_2 spectrum (Fig. 3, spectrum 1) exhibited the strong band of physically adsorbed SO_2 at 280 nm and the 215-nm signal (shoulder) of HSO_3^-. Reaction of the first increment of admitted H_2S resulted in the formation of a band around 320 nm ($S_2O_4^{2-}$, c-S_8) and a decrease in absorbance around 280 and 215 nm (spectrum 2). The latter feature indicated partial conversion of physically adsorbed SO_2 and chemisorbed HSO_3^- (compare Section 3.1). The change in absorbance around 280 and 215 nm corresponded to only a fraction of the initial absorbance due to SO_2 and HSO_3^-. Upon further admission of H_2S, the 320-nm band continued to grow and a new band at 385 nm appeared (spectrum 3). The absorbance around 280 nm, however, was reinforced.

TABLE 1

Assignments of Bands to Species Supposedly Involved in H_2S/SO_2 Interaction on NaX

UV/vis (nm)	IR (cm^1)	Species	References
—	2560	SH^-	(*3, 5, 6*)
250	—	S^{2-}	(*47, 33*)
215	1240	HSO_3^-	(*45, 46, 32*)
250	—	$S_2O_5^{2-}$	(*43, 32*)
280	1315	SO_2, physisorbed	(*46, 32, 1, 8*)
280	—	S, polymeric	(*41, 44*)
320	—	c-S_8, $S_2O_4^{2-}$	(*39, 40, 42, 43*)
385	—	S_2^{2-}	(*34, 35, 36*)

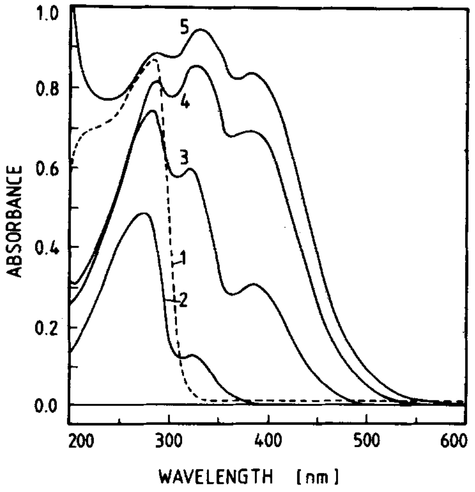

FIG. 3. UV/vis spectra after preadsorption of SO_2 onto NaX at 393 K followed by interaction with H_2S at the same temperature. (1), After uptake of 0.38 mmol g^{-1} SO_2; (2) through (5), after admission of 0.22, 0.35, 0.62, and 0.76 mmol g^{-1} H_2S, respectively.

When the ratio H_2S(admitted) : SO_2(preadsorbed) was close to 2 : 1 (spectrum 4), the decrease in absorbance around 280 nm, being the result of SO_2 conversion, was completely compensated by the absorbance of products (polymeric sulfur) in the same UV range. The change around 215 nm was less pronounced, i.e., a fraction of HSO_3^- still remained unconverted (spectrum 4 in Fig. 3). When the ratio $H_2S : SO_2 = 2$ was reached (spectrum 5), the reaction was completed, the original absorbance between 215 and 300 nm was entirely regained, and the bands left in the spectrum were those of products, in particular at 320–330 nm ($S_2O_4^{2-}$, c-S_8) and 385 nm (S_2^{2-}). The continuous increase in absorbance below 250 nm was due to the formation of water.

Combination of the UV/vis spectroscopic measurements with those in the IR region (Fig. 4) provided additional information about the interaction of H_2S and SO_2. At 393 K, the IR spectrum (Fig. 4 and Table 1) showed OH bands at 3650 and 3635 cm^{-1}, a

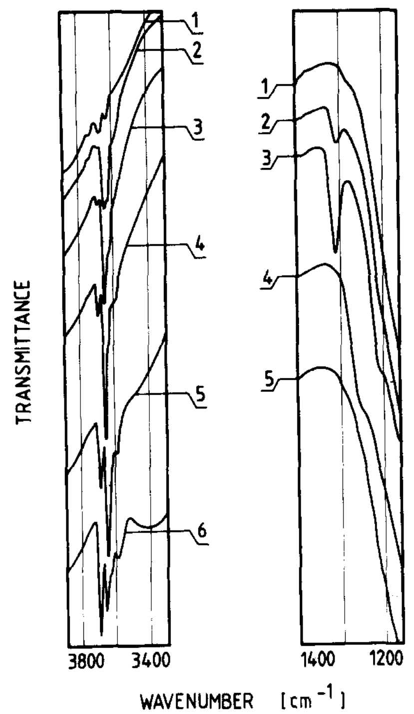

FIG. 4. IR spectra after activation of NaX, adsorption of SO_2, and interaction of SO_2 and H_2S at 393 K. (1), After activation of the wafer at 625 K; (2) and (3), after adsorption of 0.34 and 0.57 mmol g^{-1} SO_2, respectively, at 393 K; (4) through (6), after subsequent admission of 0.23, 0.57, and 1.14 mmol g^{-1} H_2S, respectively, at 393 K.

band at 1315 cm^{-1} due to physically adsorbed SO_2 (*1, 8, 9*), and a shoulder around 1240 cm^{-1} (chemisorbed SO_2). Figures 3 and 4 and Table 2 demonstrate that admission of H_2S to the catalyst preloaded with SO_2 at 393 K resulted in the

(i) decrease in intensity of the 280-nm and disappearance of the 1315-cm^{-1} signals (physically adsorbed SO_2),

(ii) decrease in intensity of the band around 215 nm band and disappearance of the shoulder around 1240 cm^{-1} (both due to chemisorbed HSO_3^-, see Refs. (*31*) and (*32*));

(iii) growth of the IR bands at 3650 and 3635 cm^{-1} (indicating acidic OH groups, compare Refs. (*31, 32, 49*));

(iv) formation of a band at 3590 cm^{-1} (due to hydrogen bonding between acidic OH groups and H_2O);

(v) appearance of the band of physically adsorbed H_2O at 1645 cm^{-1} (not shown in Fig. 4).

It seems that physisorbed SO_2 is, to some extent, converted into HSO_3^-. This view is supported by the observation that upon lower H_2S admission the shoulder around 1240 cm^{-1} remained and the bands of acidic OH groups continued to grow. The conversion of SO_2 according to Eq. (6),

$$SO_2 + H_2O \rightarrow HSO_3^- + H^+, \qquad (6)$$

might be readily assisted by some water

TABLE 2

Infrared Study of the Claus Reaction at 393 K with Preadsorption of SO_2 at 393 K on NaX Zeolite

No.	Cumulative reactant admission	Maximum absorbances of the IR bands at wavenumbers (cm^{-1})						
		3690	3650	3635	3590	1645	1315	1240
1.1	SO_2 : 0.09 mmol g^{-1}	—	0.03	0.04	Shoulder	—	—	
1.2	SO_2 : 0.18 mmol g^{-1}	—	0.07	0.07	Shoulder	—	Shoulder	
1.3	SO_2 : 0.36 mmol g^{-1}	0.02	0.12	0.08	0.01	—	0.04	
2.1	H_2S : 0.18 mmol g^{-1}	0.05	0.26	0.08	0.02	0.05	—	Shoulder
2.2	H_2S : 0.36 mmol g^{-1}	0.11	0.15	0.10	0.02	0.12	—	
2.3	H_2S : 0.53 mmol g^{-1}	0.17	0.13	0.07	0.04	0.18	—	
2.4	H_2S : 0.70 mmol g^{-1}	0.21	0.12	0.06	0.05	0.24	—	Shoulder

formed via the Claus reaction (see Eq. (2) and Ref. (*49*)). Simultaneously, the formation of protons caused the observed increase of the density of acidic OH groups.

Figure 4 and Table 2 demonstrate that further admission of H_2S brought about a steady increase of the bands of chemisorbed and physisorbed water and a decrease of the bands of acidic OH groups as a result of increasing hydrogen bonding to adsorbed product H_2O. The UV spectra (Fig. 3) showed a remarkable growth of the product bands at 320 ($S_2O_4^{2-}$, c-S_8) and 385 nm (S_2^{2-}). It seemed that the formation of HSO_3^- upon the admission of H_2S facilitated the conversion of the subsequent H_2S portions.

Subsequent thorough evacuation at 573 K resulted in the spectrum of Fig. 5 with bands around 250 (S^{2-}, see Ref. (*33*)), 295 (S_2), and 385 nm (S_2^{2-}, see Section 3.1), a very prominent band at 430 nm (S_3), and a shoulder at about 500 nm (S_4). The tentative assignments of the bands at 295, 430, and 500 to S_2, S_3, and S_4 species, respectively, were based on the work of Meyer *et al.* (*41*), who found that above 523 K c-S_8 sulfur (band at 320 nm) transforms into sulfur chains. This conversion is more pronounced the higher the temperature.

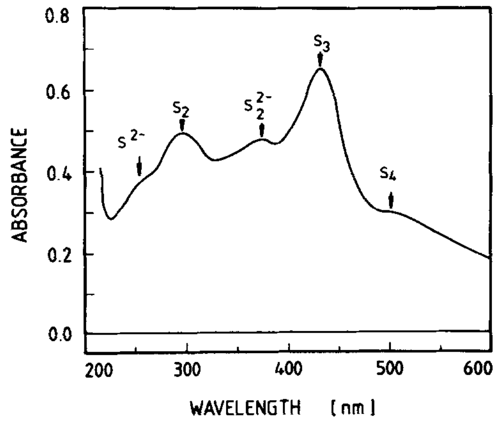

FIG. 5. UV/vis spectrum after preadsorption of 0.38 mmol g^{-1} SO_2 onto NaX, admission of 0.7 mmol g^{-1} H_2S (compare Fig. 3) and subsequent evacuation at 573 K.

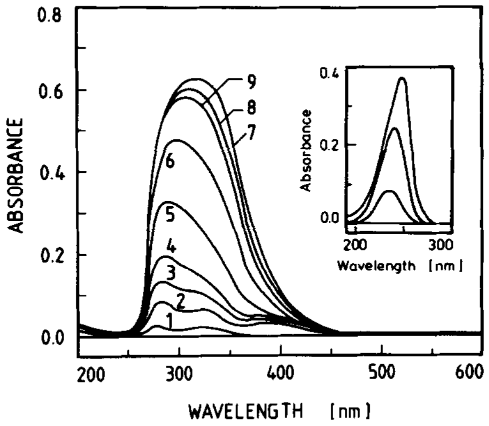

FIG. 6. UV/vis spectra after preadsorption of H_2S at r.t. and subsequent SO_2 admission. Inset: After admission of 0.02, 0.05, and 0.14 mmol g^{-1} H_2S, respectively; compare Ref. (*33*); zero line of Fig. 6 established after preadsorption of 0.37 mmol g^{-1} H_2S at r.t; spectra (1) through (7), difference spectra after admission of 0.02, 0.06, 0.09, 0.13, 0.21, 0.28, and 0.36 mmol g^{-} SO_2, respectively; (8) and (9), spectra scanned 15 and 30 min, respectively, after (7).

3.3. H_2S Preadsorption at Room Temperature (r.t.) and 393 K Followed by SO_2 Interaction at r.t.

When a NaX wafer was loaded with H_2S at r.t. and subsequently contacted with SO_2, changes in the UV/vis spectrum occurred very slowly. Only after prolonged contact time, i.e., 15 h at r.t., did product bands appear. This was in contrast to the experiment with the reversed sequence of reactant admission (Section 3.1), in which the reaction started immediately and product bands quickly developed.

Upon H_2S adsorption on NaX at r.t., a band due to S^{2-} (*33*) was observed at 250 nm. The H_2S spectrum was subtracted from all subsequent spectra, i.e., a new zero line was established. Figure 6 shows a set of difference spectra obtained after SO_2 admission to a NaX wafer, preloaded with H_2S. As in the experiments with inverse reactant admission, i.e., reaction of H_2S with preadsorbed SO_2 (see Sections 3.1 and 3.2), bands at 280, 320, and 385 nm developed, indicating the formation of reaction products and intermediates, viz., polymeric sulfur, $S_2O_4^{2-}$, c-S_8, and S_2^{2-}. After a contact time of 2 h the difference spectrum consisted of only one broad band, centered around 320 nm. Obviously, c-S_8 then predominated, but after evacuation at r.t., bands at 280 and 385 nm appeared better resolved, showing that polymeric sulfur and S_2^{2-} species were still present. The density of these species increased further when H_2S was readmitted.

While in these experiments, with preadsorption of H_2S at r.t., the reaction with subsequently admitted SO_2 seemed very slow, the situation completely changed when, prior to reaction, H_2S was contacted with the catalyst at higher temperatures.

Spectrum 1 in Fig. 7 was obtained after adsorption of 0.36 mmol g^{-1} H_2S onto a NaX wafer. It showed the band of S^{2-} at 250 nm and corresponded to the inserted spectrum of Fig. 6. When the sample, preloaded with H_2S, was subsequently heated at 393 K for 1.5 h and then cooled to r.t., no significant changes in comparison to spectrum 1 were observed. In fact, spectra 1 and 2 almost coincided. However, when 0.18 mmol g^{-1} SO_2 was added at r.t., the bands of polymeric sulfur (280 nm) and S_2^{2-} (385 nm) immediately started to develop (spectrum 3 in Fig. 7). The band at 280 nm most probably did not originate from physisorbed or weakly chemisorbed SO_2 because it grew considerably upon further conversion of H_2S at 393 K (see below) and, moreover, the IR spectra, obtained concomitantly from the same sample, did not show any band around 1315 cm^{-1}. Thus, the band is probably due to product species, viz., polymeric sulfur. Upon subsequent heating to 393 K, the conversion was even more pronounced and, besides the 280- and 385-nm bands, the spectrum (line 4 in Fig. 7) exhibited the band at 320 nm ($S_2O_4^{2-}$, c-S_8). The shoulder around 250 nm, which originated from dissociation of H_2S into S^{2-} and $2H^+$, was also still present, in agreement with the earlier observation that S^{2-} does not react with SO_2 (*33*). The species responsible for the observed bands were quite stable, i.e., they persisted even after 1 h evacuation at 473 K. Only after 9 h evacuation was a considerable decrease in intensity of all the respective bands measured and a conversion of S_2 and c-S_8 into sulfur chains indicated by increasing absorbance above 400 nm (Fig. 7, curve 5).

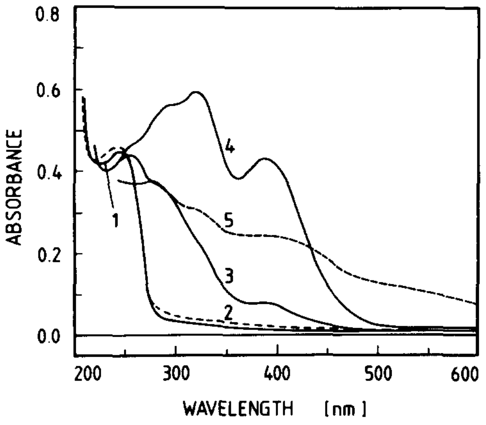

FIG. 7. UV/vis spectra after treatment of preadsorbed H_2S at 393 K and subsequent SO_2 admission. (1), After H_2S adsorption (0.36 mmol g^{-1}) at r.t.; (2), after subsequent heating to 393 K; (3), after admission of 0.18 mmol g^{-1} SO_2 at r.t.; (4), after subsequent heating to 393 K; (5), after 9 h evacuation at 493 K.

The experiments described above demonstrated that heating of the NaX wafer after loading it with H_2S obviously enhanced the reactivity of H_2S toward SO_2. A similar effect was observed when the NaX/H_2S wafer was exposed to the IR beam, where it reached a temperature of about 373 K. This had been measured by tiny thermocouples pressed into the wafer (*48*). Figure 8 presents (1) the UV spectrum after adsorption of 0.36 mmol g^{-1} of H_2S at r.t., (2) the UV spectrum after exposure to the IR beam, the IR spectrum (A, inset) with the HS^- band at 2560 cm^{-1} (*5, 6*), (3) the UV spectrum after admission of 0.18 mmol g^{-1} SO_2 at room temperature, the IR spectrum (A′, inset) after SO_2 admission and, finally, the UV/vis spectra (4) after the sample was heated in the IR beam and (5) evacuated at 573 K.

Again, the spectra clearly show that

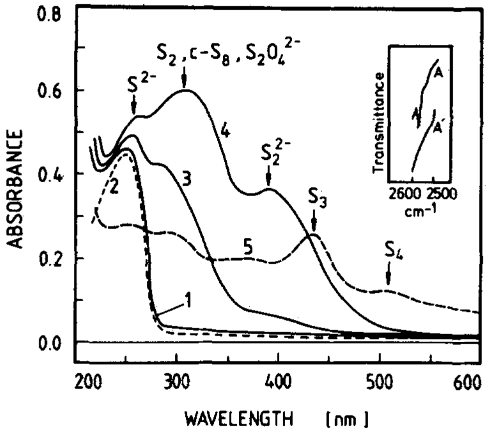

FIG. 8. UV/vis spectra after treatment of preadsorbed H_2S in the IR beam and subsequent SO_2 admission. (1), After adsorption of 0.36 mmol g^{-1} H_2S at r.t.; (2), after treatment of the sample in the IR beam for 1.5 h, where it reached a temperature of about 373 K and gave rise to the IR spectrum A (see inset); (3), after admission of 0.18 mmol g^{-1} SO_2 at r.t.; (4), after treatment of the sample for 1 h in the IR beam, yielding the IR spectrum A' (see inset); (5), after subsequent 3 h evacuation at 573 K.

there is no difference between the absorbance in UV/vis before and after the exposure of the NaX/H_2S sample to the IR beam. However, this exposure markedly accelerated the conversion upon subsequent admission of SO_2 (spectrum 3). Moreover, another exposure to the IR beam caused further growth of the UV/vis product bands. Simultaneously, the IR spectra provide evidence for the reaction of HS^- with SO_2 (see inset, A → A'), in agreement with earlier results (*8, 33*).

Obviously, the higher temperature obtained intermittently by the NaX/H_2S system, either by heating the cell or by illuminating the wafer by IR, somehow activated the species derived from preadsorbed H_2S. However, it is difficult to specify how this activation occurs. The UV/vis spectrum does not show any alteration upon temperature change or IR treatment. Measurements in the IR region, on the other hand, unavoidably require exposure of the H_2S-loaded catalyst to the IR beam. Therefore, it is at present not possible to decide whether formation of HS^- via dissociation of H_2S (*5–7*) occurs already at r.t. or requires thermal activation. In the latter case, one would conclude that the adsorbed H_2S first must transform into HS^- to become reactive or, at least, to initiate the reaction. However, another explanation of the temperature effect could be valid as well: thermal treatment might be necessary to remove H_2S or derivatives of H_2S such as S^{2-} from sites which are required for adsorption of reactive SO_2 species. Further experiments are under way to clarify this point.

The products of the reaction between preadsorbed, thermally treated H_2S and SO_2 were the same as when the reverse sequence of reactant admission was employed: polymeric sulfur (280 nm), $S_2O_4^{2-}$, c-S_8 (320 nm), and S_2^{2-} (385 nm). As before, evacuation at 523 or 573 K removed much of these species or transformed them into chain molecules such as S_3 and S_4 (see spectrum 5 in Fig. 8).

With respect to the classic Claus reaction, where oxygen is used for the final H_2S oxidation instead of SO_2, it is interesting to note that the product species are the same as formed by the reactions described so far.

4. CONCLUSIONS

(i) Combined transmission UV-visible and IR spectroscopy is an appropriate tool for investigating adsorption and interaction of H_2S and SO_2 on zeolite catalysts for the Claus reaction.

(ii) Reactivity of HSO_3^-, formed by chemisorption of SO_2, and HS^-, formed by dissociative adsorption of H_2S, was confirmed.

(iii) Spectroscopic evidence was obtained for $S_2O_4^{2-}$, S_2^{2-} and c-S_8, polymeric S as intermediates and products of the Claus reaction, respectively.

(iv) The same products were observed irrespective of whether preadsorbed SO_2

interacted with H_2S or vice versa or whether O_2 was used as an oxidizing agent.

(v) Heating of preadsorbed H_2S on NaX to 375 K prior to interaction with SO_2 at r.t. increased the rate of reaction.

REFERENCES

1. Deo, A. V., Dalla Lana, I. G., and Habgood, H. W., *J. Catal.* **21,** 270 (1971).
2. Slager, T. L., and Amberg, C. H., *Canad. J. Chem.* **50,** 3416 (1972).
3. Förster, H., and Schuldt, M., *J. Colloid Interface Sci.* **52,** 380 (1975).
4. Förster, H., and Schuldt, M., *Spectrochim. Acta* **31A,** 685 (1975).
5. Förster, H., and Seelemann, R., *Ber. Bunsen-Ges. Phys. Chem.* **80,** 153 (1976).
6. Karge, H. G., and Raskó, J., *Proc. 3rd Int. Symp. Heterog. Catal., Varna, Bulgaria, 1975* (D. Shopov, A. Andreev, A. Palazov, and L. Petrov, Eds.), p. 615. Publ. House Bulg. Acad. Sci., Sofia, 1978.
7. Karge, H. G., and Raskó, J., *J. Colloid Interface Sci.* **64,** 522 (1978); *Magy. Kem. Foly.* **84,** 109 (1978).
8. Karge, H. G., and Ladebeck, J., *Proc. 5th Int. Conf. Zeolites, Naples, 1980,* Recent Progress Reports and Discussion (R. Sersale, C. Colella, and R. Aiello, Eds.), p. 180. Giannini, Naples, 1980.
9. Karge, H. G., Ladebeck, J., and Nag, N. K., *Prepr. 7th Canad. Symp. Catal., Edmonton, Canada, 1980* (S. E. Wanke and S. K. Chakrabartty, Eds.), p. 225. Canadian Society of Chemical Engineering, 1980.
10. Lavalley, J. C., Travert, J., Chevreau, Th., Lamotte, J., and Saur, O., *J. Chem. Soc. Chem. Commun.*, p. 146 (1979).
11. Lavalley, J. C., Janin, A., and Preud'homme, J., *React. Kinet. Catal. Lett.* **18,** 85 (1981).
12. Saur, O., Chevreau, Th., Lamotte, J., Travert, J., and Lavalley, J. C., *J. Chem. Soc. Faraday Trans. I* **77,** 427 (1981).
13. Lavalley, J. C., Lamotte, J., Saussey, H., and Preud'homme, J., *Sulfur Lett.* **1,** 101 (1982).
14. Lavalley, J. C., Lamotte, J., Saur, O., Mohammed Saad, A. B., Tripp, C., and Morrow, B. A., *Proc. Int. Conf. Fourier and Computerized Infrared Spectrosc., Ottawa, 1985* (J. G. Grasselli and D. G. Cameron, Eds.), Vol. 553. SPIE (Society of Photooptical Instrumentation Engineers), Bellingham, Washington, p. 486, 1985.
15. Lavalley, J. C., Mohammed Saad, A. B., Tripp, C. P., and Morrow, B. A., *J. Phys. Chem.* **90,** 980 (1986).
16. Datta, A., Cavell, R. G., Tower, R. W., and George, Z. M., *J. Phys. Chem.* **89,** 443 (1985).
17. Datta, A., and Cavell, R. G., *J. Phys. Chem.* **89,** 450 (1985).
18. Datta, A., and Cavell, R. G., *J. Phys. Chem.* **89,** 454 (1985).
19. Chang, C. C., *J. Catal.* **53,** 374 (1978).
20. Karge, H. G., Tower, R. W., Dudzik, Z., and George, Z. M., *Proc. 7th Int. Congr. Catal., Tokyo, 1980* (T. Seiyama and K. Tanabe, Eds.), p. 643. Kodansha/Elsevier, Tokyo/Amsterdam, 1980.
21. Karge, H. G., and Dalla Lana, I. G., *J. Phys. Chem.* **88,** 1538 (1984).
22. Karge, H. G., Dalla Lana, I. G., Trevizan de Saurez, S., and Zhang, Y., *Proc. 8th Int. Cong. Catal., Berlin, 1984,* Vol. III, p. 453. Verlag Chemie, Weinheim, 1984.
23. Karge, H. G., Zhang, Y., Trevizan de Suarez, S., and Ziołek, M., *Proc. Conf. Structure and Reactivity of Modified Zeolites, Prague, 1984* (P. A. Jacobs *et al.*, Eds.), p. 49. Elsevier, Amsterdam, 1984.
24. Ben Taarit, Y., Naccache, C., and Che, M., *Chem. Phys. Lett.* **24,** 41 (1973).
25. Ono, Y., Suzuki, K., and Keii, T., *J. Phys. Chem.* **78,** 218 (1974).
26. Ono, Y., Tokunaga, H., and Keii, T., *J. Phys. Chem.* **79,** 752 (1975).
27. Dudzik, Z., and Bilska-Ziołek, M., *Bull. Acad. Pol. Sci., Ser. Sci. Chim.* **23,** 699 (1975).
28. Khulbe, K. C., and Mann, R. S., *J. Catal.* **51,** 364 (1978).
29. Muha, G. M., *J. Catal.* **58,** 478 (1979).
30. Khulbe, K. C., Mann, R. S., and Manoogian, A., *Zeolites,* **3,** 360 (1983).
31. Karge, H. G., Trevizan de Suarez, S., and Dalla Lana, I. G., *J. Phys. Chem.* **88,** 1782 (1984).
32. Karge, H. G., Łaniecki, M., and Ziołek, M., *Proc. 7th Int. Zeolite Conf., Tokyo, 1986* (Y. Murakami, A. Iijima, and J. W. Ward, Eds.), p. 617. Kodansha, Tokyo and Elsevier, Amsterdam, 1986.
33. Karge, H. G., Ziołek, M., and Łaniecki, M., *Zeolites* **7,** 197 (1987).
34. McLaughlan, S. D., and Marshall, D. J., *J. Phys. Chem.* **74,** 1359 (1970).
35. Wieckowski, A., *Phys. Status Solidi* **42,** 125 (1970).
36. Chivers, T., and Drummond, I., *Chem. Soc. Rev.* **2,** 233 (1973).
37. Barr, J., Gillespie, R. J., and Ummat, P. K., *J. Chem. Soc. Chem. Commun.*, p. 264 (1970).
38. Giggenbach, W. F., *J. Chem. Soc. Chem. Commun.*, p. 852 (1970).
39. Eriksen, T. E., *J. Chem. Soc. Faraday Trans. I* **70,** 208 (1974).
40. Meyer, B., and Spitzer, K., *J. Phys. Chem.* **76,** 2274 (1972).

41. Meyer, B., Oommen, T. V., and Jensen, D., *J. Phys. Chem.* **75,** 912 (1971).
42. Oommen, T. V., Ph.D. Thesis, University of Washington, Seattle, 1970.
43. Hayon, E., Treinin, A., and Wilf, J., *J. Amer. Chem. Soc.* **94,** 47 (1972).
44. Meyer, B., Stroyer-Hansen, T., Jensen, D., and Oommen, T. V., *J. Amer. Chem. Soc.* **93,** 1034 (1971).
45. Golding, R. M., *J. Chem. Soc. Chem. Commun.,* p. 3711 (1960).
46. Huss, A., and Eckert, C. A., *J. Phys. Chem.* **81,** 2266 (1977).
47. Giggenbach, W., *Inorg. Chem.* **10,** 1333 (1971).
48. Karge, H. G., and Klose, K., *Z. Phys. Chem. Neue Folge* **83,** 92 (1973).
49. Łaniecki, M., Ziołek, M., and Karge, H. G., *J. Phys. Chem.* **91,** 4 (1987).